17th World Conference on Earthquake Engineering, 17WCEE
Sendai, Japan - September 13th to 18th 2020
Paper N° C002724
Registration Code: S-A02193

SELECTING THREE COMPONENTS OF GROUND MOTIONS FROM CONDITIONAL SPECTRA FOR MULTIPLE STRIPE ANALYSES

N. S. Kwong [1], K. S. Jaiswal [2], N. Luco [3], J. W. Baker [4]

[1] *Research Civil Engineer, U.S. Geological Survey, nkwong@usgs.gov*
[2] *Research Structural Engineer, U.S. Geological Survey, kjaiswal@usgs.gov*
[3] *Research Structural Engineer, U.S. Geological Survey, nluco@usgs.gov*
[4] *Professor, Stanford University, bakerjw@stanford.edu*

Abstract

For complex structures where the seismic response depends appreciably on the vertical (V) component of ground motion (GM) (e.g., base-isolated buildings, long-span bridges, dams, nuclear power plants), incremental dynamic analysis (IDA) is commonly utilized to estimate seismic risk, where the V components of GM are selected and scaled based on the corresponding horizontal (H) components. The resulting seismic risk (e.g., fragility estimates, annual rates of failure) will likely be significantly biased when the scale factors in IDA are very large. As an alternative to IDA, multiple stripe analyses (MSA) with GMs for each stripe selected from the Conditional Spectrum (CS) can be used to estimate the seismic risk; however, the V components are still commonly selected and scaled based on the corresponding H components. Consequently, these V components may still be inconsistent relative to the corresponding target hazard, again yielding biased estimates of seismic risk. To improve the accuracy of seismic risk estimates, we extend the CS to include the V component of GM and present an approach to select multicomponent GMs that are hazard consistent with respect to all three components of GM. Using the target and the GM selection approach developed in this study, we then evaluate typical current practice for selecting and scaling V components of GM. We observe that the latter approach can yield hazard-inconsistent multicomponent GMs, but hazard consistency can be improved by including the V component in the selection process, constraining the scale factors, or widening the period range for selecting GMs.

Keywords: ground motion selection; Conditional Spectrum; vertical components; nonlinear response history analysis

1. Introduction

Nonlinear response history analyses [1], or dynamic structural analyses, are often required for comprehensive risk-based assessments [2] of complex structures. In this context, the seismic risk of the structure (e.g., its annual probability of collapse) is estimated by assessing the response of a finite-element model of the structure when subjected to input ground acceleration time histories, or ground motions (GMs) for brevity. Consequently, the estimated seismic risk depends significantly on the input GMs.

For risk-based assessments, two methods are often used to develop such input GMs: (i) incremental dynamic analyses (IDA) [3] or (ii) multiple stripe analyses (MSA) [4]. In both methods, a single intensity measure (IM) is first chosen to quantify the severity of the seismic excitation (e.g., spectral acceleration at the structure's fundamental period). In IDA, a single ensemble of seed GMs is scaled continuously to different levels of the chosen IM, yielding an ensemble of response-vs-IM curves that capture the structure's behavior from elastic response to complete failure; in contrast, different ensembles of GMs are selected and scaled to different discrete levels of the IM in MSA, yielding a set of seismic demands per discrete IM level, which looks like multiple "stripes" when plotting seismic demand against discrete IM levels [5]. Moreover, the ensemble of seed GMs for IDA is often selected using engineering judgment [6] whereas the ensemble of GMs for a given IM level in MSA is often selected to agree with the Conditional Spectrum (CS) [7]–[10], which is derived from the seismic hazard for the site.

When estimating annual rates of collapse or developing fragility functions for complex structures where the seismic response depends appreciably on the vertical (V) component of GM (e.g., base-isolated buildings [11], long-span bridges [12], dams [13], nuclear power plants [14]), IDA is more commonly utilized than MSA [15]–[17]. Furthermore, the multicomponent GMs for IDA are selected and scaled based on the horizontal (H) components, where the corresponding V components are scaled by the same scale factors that were applied to the H components [2], [18]. When scale factors in IDA are very large, which depends on the strength of the structure as well as the return periods of interest, the resulting seismic risk will likely be significantly biased [19]–[22].

Although MSA with CS exists as an alternative to IDA, the V components are still commonly selected and scaled based on the corresponding H components. Consequently, these V components may still be inconsistent relative to the corresponding target hazard, again yielding biased estimates of seismic risk. Moreover, practical tools and guidance for explicitly including the V component of GM into the CS do not exist, even though the V component has been included into the Conditional Mean Spectrum (CMS) [23], [24] and the CS has been recently extended for two H components of GM [25], [26]. In order to develop such guidance and evaluate the existing approaches for selecting V components, the target spectrum for the V component of GM must first be developed.

In this paper, the CS is extended to include the V component of GM, and the necessary GM models for practical implementation are explicitly identified, informing future work on developing GM prediction models (GMPMs), correlation models, and a U.S. Geological Survey (USGS) web-based tool. Furthermore, an approach to select multicomponent GMs that are hazard consistent [8] with respect to spectral accelerations for all three components of GM is presented. Using the target spectrum and the GM selection approach developed in this study, typical aspects of current practice for selecting and scaling V components of GM are evaluated. As will be presented later, the typical current practice can yield hazard-inconsistent multicomponent GMs, but hazard consistency can be improved by including the V component in the selection process, constraining the scale factors, or widening the period range for selecting GMs.

2. Including the vertical component of ground motion into the Conditional Spectrum

To include the V component of GM, the logarithms of spectral accelerations at different vibration periods are assumed to jointly follow a multivariate normal distribution for a given earthquake scenario (i.e., known magnitude M and source-to-site distance R) [27]. Specifically, for the kth component of GM, where $k = H$ or V, the mean vector $\boldsymbol{\mu}$ and covariance matrix $\boldsymbol{\Sigma}$ of this "unconditional distribution" [10], [28] are expressed as:

$$\boldsymbol{\mu} = \boldsymbol{\mu}^{(k)} \qquad \boldsymbol{\Sigma} = \boldsymbol{\Sigma}^{(k,k)} \tag{1}$$

where the ith element of $\boldsymbol{\mu}^{(k)}$ and the ijth element of $\boldsymbol{\Sigma}^{(k,k)}$ are respectively given by:

$$\mu_i^{(k)} = \ln\left[A_{k,m}(T_i)\right] \qquad \Sigma_{ij}^{(k,k)} = \sigma_k(T_i)\sigma_k(T_j)\rho_{k,k}(T_i, T_j) \tag{2}$$

$A_{k,m}(T_i)$ and $\sigma_k(T_i)$ denote, respectively, the median spectral acceleration and logarithmic standard deviation at vibration period T_i for the kth component of GM, which can be obtained from standard GMPMs. (Note that the abbreviation GMPM has been used to distinguish from correlation models when discussing GM models.) The correlation coefficient between spectral accelerations at T_i and T_j for the kth component of GM, $\rho_{k,k}(T_i, T_j)$, can be obtained from a correlation model.

To illustrate, consider an earthquake scenario defined by M=7 and R=10 km. Fig. 1a illustrates the resulting median spectrum $A_{H,m}$ and logarithmic standard deviation σ_H for the H component of GM, which are estimated from the GMPM after Campbell and Bozorgnia [29]. By further estimating the correlations between two different periods $\rho_{H,H}(T_i, T_j)$ using a correlation model (e.g., [30]), the multivariate normal distribution expressed in Eq. (1) is fully specified and can be used to probabilistically generate realistic response spectra for selecting H components of GM [7], [10], [28], [31]. Furthermore, the two orthogonal H components of GMs can be selected in this manner by characterizing the H component using RotD50 or another summarizing metric (e.g., see [2], [7], [32]).

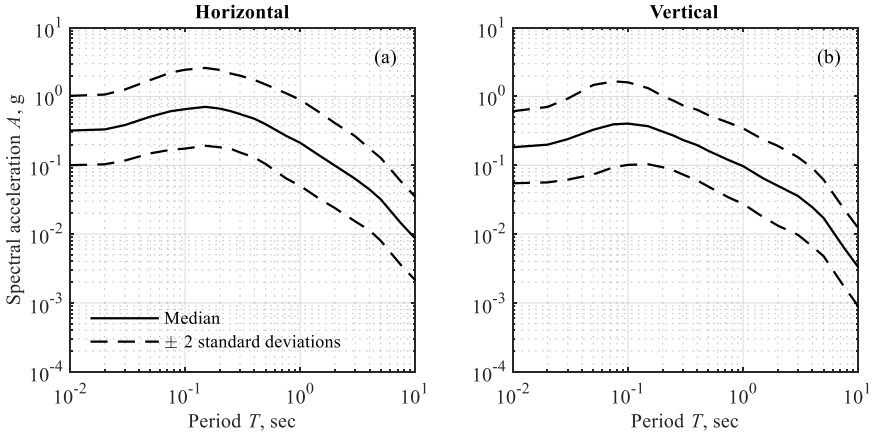

Fig. 1 – Median target spectra with ± 2 logarithmic standard deviations for an earthquake scenario defined by M=7 at R=10 km: (a) H and (b) V components of GM.

By taking advantage of the latest GMPMs from the NGAW2 project [33], the "unconditional" GM selection procedure described in the preceding paragraph can be repeated independently for the V components of GM. For example, Fig. 1b illustrates the median spectrum $A_{V,m}$ and logarithmic standard deviation σ_V for the V component of GM, which are estimated from the GMPM after Bozorgnia and Campbell [34]. By further estimating the correlations between two different periods $\rho_{V,V}(T_i, T_j)$ using the correlation model developed recently by Gülerce et al. [35], the multivariate normal distribution expressed in Eq. (1) is again fully specified and can be used to probabilistically generate realistic response spectra for selecting V components of GM; however, such ensembles of V components of GM are of limited utility because they are obtained independently from the H components and yet response history analysis requires simultaneous application of all components of GM to the finite-element model.

To include both H and V components simultaneously, the mean vector and covariance matrix from Eq. (1) are rewritten as:

$$\boldsymbol{\mu} = [\boldsymbol{\mu}^{(H)} \quad \boldsymbol{\mu}^{(V)}] \qquad \boldsymbol{\Sigma} = \begin{bmatrix} \boldsymbol{\Sigma}^{(H,H)} & \boldsymbol{\Sigma}^{(H,V)} \\ \boldsymbol{\Sigma}^{(V,H)} & \boldsymbol{\Sigma}^{(V,V)} \end{bmatrix} \tag{3}$$

where $\boldsymbol{\Sigma}^{(V,H)}$ is equal to the transpose of $\boldsymbol{\Sigma}^{(H,V)}$ and the ijth element of $\boldsymbol{\Sigma}^{(H,V)}$ is given by:

$$\Sigma_{ij}^{(H,V)} = \sigma_H(T_i)\sigma_V(T_j)\rho_{H,V}(T_i, T_j) \tag{4}$$

$\rho_{H,V}(T_i, T_j)$ denotes the correlation coefficient between spectral acceleration at period T_i for the H component of GM and spectral acceleration at period T_j for the V component of GM. Eq. (4) highlights the fact that a correlation model for $\rho_{H,V}(T_i, T_j)$ is required to fully specify the target spectrum for selecting multicomponent GMs that include the V component; a GMPM for the V component alone (e.g., [34]–[36]) is inadequate. Although the model by Baker and Cornell [31] estimates such correlations, it is applicable only for vibration periods from 0.05 to 4 sec whereas stiff structures (e.g., dams, nuclear power plants) would require estimates for shorter vibration periods, and it seems to be the only such model.

Fortunately, GMPMs for H components of GM and GMPMs for vertical-to-horizontal (V/H) ratios can be combined to derive correlations $\rho_{H,V}(T_i, T_j)$ for a wider period range. As derived in Kwong and Chopra [24], this relationship is given by:

$$\rho_{H,V}(T_i, T_j) = \frac{\sigma_H(T_j)\rho_{H,H}(T_i,T_j)+\sigma_{V/H}(T_j)\rho_{H,V/H}(T_i,T_j)}{\sqrt{\sigma_H^2(T_j)+\sigma_{V/H}^2(T_j)+2\sigma_H(T_j)\sigma_{V/H}(T_j)\rho_{H,V/H}(T_j,T_j)}} \tag{5}$$

where $\sigma_{V/H}(T_j)$ denotes the logarithmic standard deviation for the V/H ratio at period T_j and $\rho_{H,V/H}(T_i, T_j)$ denotes the correlation coefficient between spectral acceleration at period T_i for the H component of GM and V/H ratio at period T_j. Fig. 2b presents an example of correlations $\rho_{H,V}(T_i, T_j)$ that were derived by using the GMPM after Bozorgnia and Campbell [37] for estimating $\sigma_{V/H}(T_j)$ and the correlation model after Gülerce and Abrahamson [23] for estimating $\rho_{H,V/H}(T_i, T_j)$. Comparing these correlations against those from the correlation model after Baker and Cornell [31] (Fig. 2a) reveals that (i) slightly stronger correlations are obtained from Eq. (5) and (ii) $\rho_{H,V}(T_i, T_j)$ is not necessarily identical to $\rho_{H,V}(T_j, T_i)$, which can be verified by swapping the input periods in Eq. (5).

Assuming the joint distribution of the logarithms of spectral accelerations remains a multivariate normal distribution after including the H and V components of GM simultaneously per Eq. (3), the resulting conditional distribution remains multivariate normal [38]. To illustrate, let us assume that an "epsilon" at a conditioning period T^* for the H component of GM, denoted by $\varepsilon_H(T^*)$, was specified; since epsilon is defined as the number of logarithmic standard deviations between the median acceleration and the specified value [39], specifying an epsilon is equivalent to specifying a spectral acceleration at T^* for the H component of GM, which is required for each stripe in MSA. With this starting point, it can be readily shown (e.g., [24], [40]) that the resulting multicomponent CS continues to follow a multivariate normal distribution; in particular, the conditional mean vector is equal to the logarithm of the CMS for the kth component of GM:

$$A_{k,CMS}(T_i) = A_{k,m}(T_i) \cdot \exp\left[\varepsilon_H(T^*)\rho_{H,k}(T^*, T_i)\sigma_k(T_i)\right] \tag{6}$$

The conditional covariance between the logarithm of spectral acceleration at T_i for the kth component of GM and the logarithm of spectral acceleration at T_j for the lth component of GM, where $l = H$ or V, is denoted by $\tilde{\Sigma}_{\ln[A_k(T_i)],\ln[A_l(T_j)]}$ and given by:

$$\tilde{\Sigma}_{\ln[A_k(T_i)],\ln[A_l(T_j)]} = \sigma_k(T_i)\sigma_l(T_j)\left[\rho_{k,l}(T_i,T_j) - \rho_{H,k}(T^*,T_i)\rho_{H,l}(T^*,T_j)\right] \quad (7)$$

For example, when $k = l = V$ and $T_i = T_j = T$, the conditional covariance in Eq. (7) reduces to the square of the conditional standard deviation, which is equal to $\sigma_V^2(T)\left[1 - \rho_{H,V}^2(T^*,T)\right]$ because $\rho_{V,V}(T,T) = 1$.

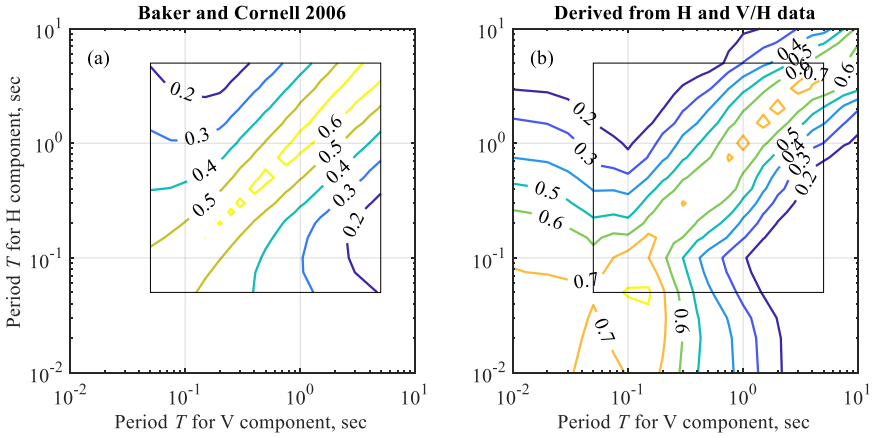

Fig. 2 – Estimates of correlation between $A_H(T)$ and $A_V(T)$ using (a) Baker and Cornell 2006 model [31] and (b) Equation 5 with models by Baker and Jayaram [30] for $\rho_{H,H}$, Campbell and Bozorgnia [29] for σ_H, Gülerce and Abrahamson [23] for $\rho_{H,V/H}$, and Bozorgnia and Campbell [37] for $\sigma_{V/H}$.

As an example, Fig. 3 presents the multicomponent CS for the case where the conditioning period T^* is equal to 1 sec and $\varepsilon_H(T^*)$ is specified as 2; the median spectra from Fig. 1 are also shown (red lines) for reference. Fig. 3b shows that the epsilon at T^* for the V component of GM, denoted by $\varepsilon_V(T^*)$ and schematically shown via the thick blue segment, is less than 2, despite $\varepsilon_H(T^*) = 2$, because the correlation between the H and V components of GM at this vibration period is less than unity. Furthermore, Fig. 3b shows that the variability in spectral accelerations at T^* for the V component of GM is only slightly reduced when $\varepsilon_H(T^*)$ is known with certainty; if the correlation $\rho_{H,V}(T^*,T^*)$ was closer to unity, then Fig. 3b would have shown a "pinch" around T^* that is similar to the one shown in Fig. 3a.

Different GM models are needed for developing the different target spectra previously presented. For example, Eq. (3) and Eq. (4) show that when developing the "unconditional distribution" for a given earthquake scenario, two types of GMPMs are needed (i.e., A_m and σ for both H and V components of GM) and three types of correlation models are needed: (i) $\rho_{H,H}(T_i,T_j)$, (ii) $\rho_{H,V}(T_i,T_j)$, and (iii) $\rho_{V,V}(T_i,T_j)$. Based on Eq. (6) and Eq. (7), this exact same set of GM models are also needed when developing the multicomponent CS. In contrast, developing a multicomponent CMS requires all the preceding GM models except for estimating $\rho_{V,V}(T_i,T_j)$, which can be seen in Eq. (6). Moreover, when a correlation model for $\rho_{H,V}(T_i,T_j)$ is unavailable, Eq. (5) can be used but it requires two additional models as surrogates: (i) a GMPM for $\sigma_{V/H}$ and (ii) a correlation model for $\rho_{H,V/H}(T_i,T_j)$.

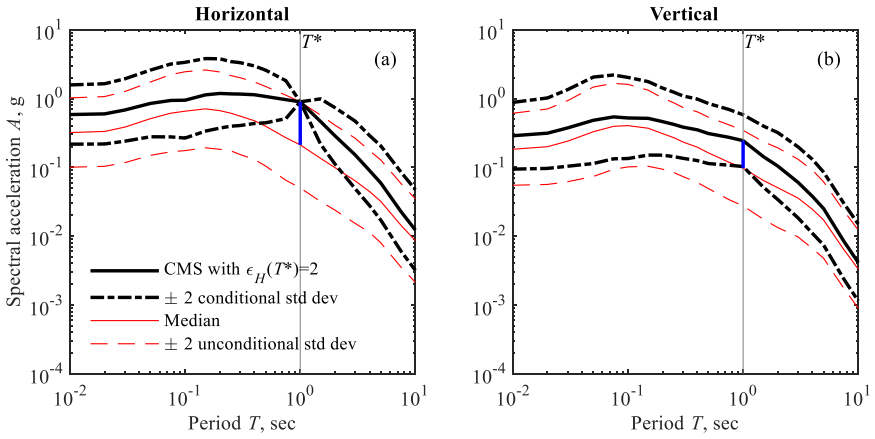

Fig. 3 – Multicomponent CS for GM scenario defined by M=7, R=10 km, and $\varepsilon_H = 2$ at $T^* = 1$ sec: (a) H and (b) V components of GM; thick blue lines schematically show ε_H and ε_V at T^*.

3. Selecting three-component ground motions to match the Conditional Spectrum

3.1 Proposed approach

As mentioned previously, the algorithm developed by Jayaram et al. [7] and Baker and Lee [10] can be used to independently select k components of GM so that the statistics of the ensemble agree closely with the target spectrum for the kth component of GM, where $k = H$ or V. First, a period range is specified for defining the target spectrum and comparing response spectra, which can vary for different components of GM (e.g., $N_{p,k} = 20$ periods logarithmically spaced between 0.05 and 10 sec). Second, Monte Carlo simulation is used to probabilistically generate synthetic response spectra from the target spectrum. Third, each synthetic spectrum is used as a temporary target spectrum, $A_{k,TS}(T)$, to find the best GM (among all screened candidates in the GM database) whose original response spectrum, $A_{k,0}(T)$, agrees most closely to the target after it has been scaled by a scale factor, denoted by SF_k; this comparison is quantified using a sum-of-squared differences (SSD) over the period range discretized by $N_{p,k}$:

$$SSD_k = \sum_{j=1}^{N_{p,k}} \left(\ln\left[SF_k \times A_{k,0}(T_j)\right] - \ln\left[A_{k,TS}(T_j)\right]\right)^2 \tag{8}$$

Finally, this initial ensemble of GMs is optimized using a "greedy technique" [7] so that the statistics of the final ensemble of GMs agree more closely with the specified target spectrum.

Special considerations are required when modifying the preceding algorithm to include the V component of GM simultaneously with the H components. First, the period range for comparing response spectra of the V components can, in general, differ from that used for the H components (e.g., Section C17.3.3 of ASCE/SEI 7-16 [41] states $0.2T_v$ to $1.5T_v$ for V component and Section 16.2.3.1 of the same reference states T_{90mp} to $2T_1$ for H components, where T_{90mp} refers to the modal period corresponding to 90% mass participation). Second, the scale factor for the H components can also, in general, differ from that for the V component [12], [41]; e.g., the H component can be scaled to match $A_{H,TS}(T^*)$ while the V component can be scaled using a factor of $SF_{V,opt}$ to optimally (i.e., minimizing SSD_V) match the corresponding target over a period range [24]:

$$SF_{V,opt} = \left[\prod_{j=1}^{N_{p,V}} \frac{A_{V,TS}(T_j)}{A_{V,0}(T_j)}\right]^{1/N_{p,V}} \tag{9}$$

Third, the comparison of GM spectra for the H components must be conducted simultaneously for the V component; one way to achieve this is by introducing a weight for the H component, w_H, to compute a combined SSD [24], [42]:

$$SSD_{combined} = w_H SSD_H + (1 - w_H) SSD_V \quad (10)$$

When applying the "greedy technique" for only H components of GM, an additional SSD must be computed for a given GM ensemble to measure the discrepancy between both means and variances (denoted as SSE_s in Equation 2 of Jayaram et al. [7]). When including the V component, this "ensemble SSD" is revised by first computing it for H and V components separately and then combining the two using Eq. (10). Finally, the conditional covariance matrix in Eq. (7) must be checked for positive definiteness to enable probabilistic generation of synthetic response spectra. In practice, an approximate covariance matrix [43] can be used to guarantee this property. These considerations are incorporated into the GM selection algorithm by Jayaram et al. [7] and Baker and Lee [10] as a new version of the software on GitHub.

Among the different choices for user inputs into the software, we propose to select multicomponent GMs by following three key guidelines: (i) including the V component during the selection process, (ii) constraining the scale factors as much as possible, and (iii) comparing response spectra with a period range as wide as possible. For example, Fig. 4 compares the statistics of 30 selected GMs against the multicomponent CS from Fig. 3, for the case where: (i) $w_H = 0.5$ was used for Eq. (10), (ii) separate scale factors (all constrained to within 0.25 to 4) were used for the V components, and (iii) the same period range of 0.01 to 10 sec (150 periods logarithmically spaced) was used for both H and V components. As shown in the figure, both the geomean and the logarithmic standard deviations of the selected GMs agree closely with the target for both H and V components of GM at periods from 0.01 to 10 sec.

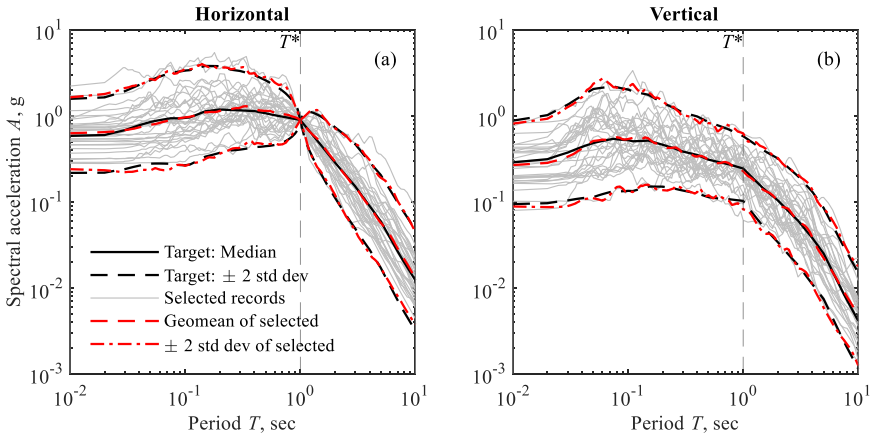

Fig. 4 – Records selected and scaled to match the CS for both H and V components of GM at periods from 0.01 to 10 sec with scale factors constrained to within 0.25 to 4: (a) H and (b) V components of GM.

The GM selection approach described in the preceding paragraph will likely improve the accuracy of seismic risk estimates for complex structures. In general, the accuracy of risk estimates depends on the hazard consistency of the input GMs with respect to IMs that are "sufficient" [20], [44]–[47]; however, it is rare for simple IMs (e.g., spectral accelerations over a narrow period range for the H component of GM) to be truly "sufficient" for complex structures [45]. Fortunately, ensuring hazard consistency with respect to spectral accelerations over a wide period range for all three components of GM (Fig. 4) seems to improve hazard consistency with respect to other IMs as well.

To illustrate, hazard consistency of the selected GMs with respect to 5-75% significant duration, D_{5-75} [48], is shown in Fig. 5. This metric is chosen to represent cumulative effects of the GM since (i) the proposed CS approach does not guarantee hazard consistency with respect to such cumulative effects, and at

the same time, (ii) a GM is fully characterized by including cumulative effects in addition to intensity and frequency content [49]. Using the Generalized Conditional Intensity Measure (GCIM) method [50], the GMPM for D_{5-75} after Bommer et al. [48], and the correlation model for $\rho_{A_H,D_{5-75}}$ after Bradley [51], the target conditional distribution of D_{5-75} for individual H components of GM is derived and shown in Fig. 5a-b (green). Since similar GM models are unavailable for the V component of GM, the target shown in Fig. 5c was approximated (and hence colored red) by first computing the necessary statistics for D_{5-75} (i.e., median, logarithmic standard deviation, and correlation) from 30 unmodified multicomponent GMs before applying the GCIM method. These unmodified GMs were selected to match the unconditional distribution for the earthquake scenario (shown in Fig. 1) using the approach proposed in this paper (i.e., $w_H = 0.5$, scale factors constrained to unity, and period range of 0.01 to 10 sec for comparing GM spectra); the reader is referred to Kwong and Chopra [24] for reasons why 0.5 was chosen among other values for w_H.

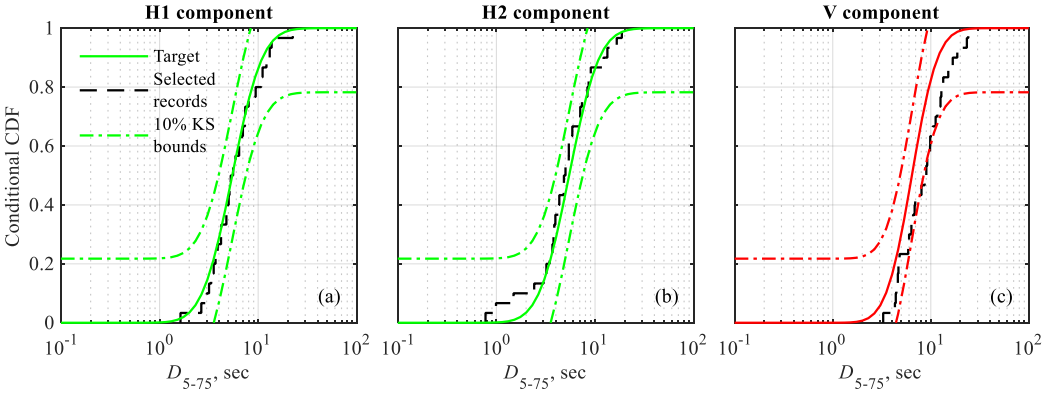

Fig. 5 – Evaluation of 5-75% significant duration, D_{5-75}, for selected records whose spectra are shown in Fig 4: (a) H1, (b) H2, and (c) V components of GM.

By superimposing the values of D_{5-75} from the scaled GMs against the corresponding targets and supplying 10% Kolmogorov-Smirnov (KS) bounds, which are more stringent than 5% bounds, it is evident from Fig. 5a-b that the selected GMs are also hazard consistent with respect to D_{5-75} for the H components of GM despite D_{5-75} not being used to select the GMs. Although the empirical CDF for the V component falls slightly outside of the KS bounds (Fig. 5c), the discrepancy is slight, especially since the target for the V component was approximated due to a lack of GM models. Interestingly, these selected GMs were also hazard consistent with respect to D_{5-95}, PGA, and PGV (not shown due to space limitations), suggesting that the GM selection approach proposed in this paper improves the accuracy of the resulting seismic risk estimates.

3.2 Typical current practice

The current practice for selecting V components of GM differs from the approach described in the previous subsection in three typical ways. First, V components are almost always obtained by first selecting the H components and then using the corresponding V components (i.e., V components are excluded during selection process) [2], [18], [41]. Second, the V components are typically scaled by the same scale factors that were applied to the H components; moreover, large scale factors are usually employed when conducting IDA or when not enough GMs are available in the database for selection [15], [17]. Third, the period range suggested for comparing response spectra usually spans roughly an order of magnitude (e.g., see [41]).

To evaluate these three aspects that are typical of current practice, a different ensemble of multicomponent GMs was selected and examined for hazard consistency. Specifically, H components of GMs are selected to match the same multicomponent CS from Fig. 3 over a period range of 0.2 to 2 sec (i.e., $w_H = 1$), and the corresponding V components are simply scaled by the same scale factors that were identified for the H components; all scale factors are unconstrained. The response spectra of these selected GMs are presented in Fig. 6. As expected, the selected GMs are hazard consistent with respect to spectral accelerations from 0.2 to 2 sec for the H components of GM (Fig. 6a); however, they are hazard inconsistent with respect to

spectral accelerations elsewhere (in particular, for the V component of GM at periods longer than 0.2 sec as shown in Fig. 6b). Furthermore, these selected GMs are also hazard inconsistent with respect to D_{5-75}, as demonstrated by the solid red curves in Fig. 7. Since it is unlikely that spectral accelerations over a narrow period range for the H component of GM will be truly "sufficient" for the seismic response of 3D complex structures [45], [50], the preceding hazard inconsistencies suggest that resulting estimates of seismic risk would be biased.

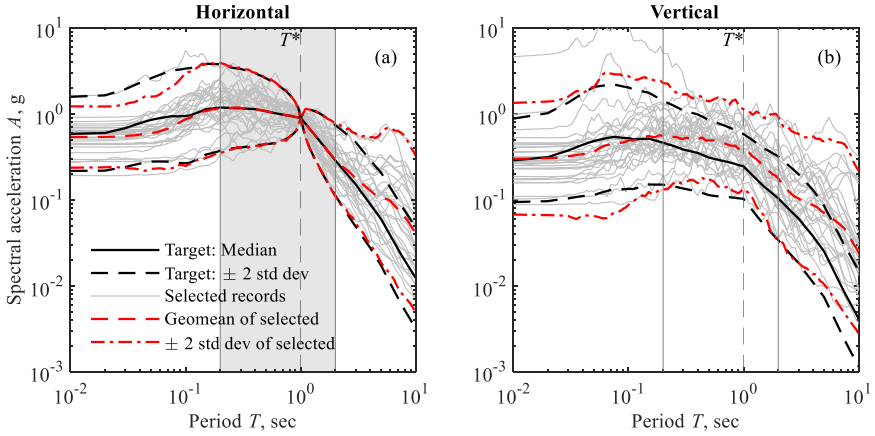

Fig. 6 – (a) Records selected and scaled to match the CS only for the H component of GM at periods from $0.2T^*$ to $2T^*$ (shaded region) with (b) corresponding V components scaled by the same scale factors that were applied to the H components; all scale factors are unconstrained.

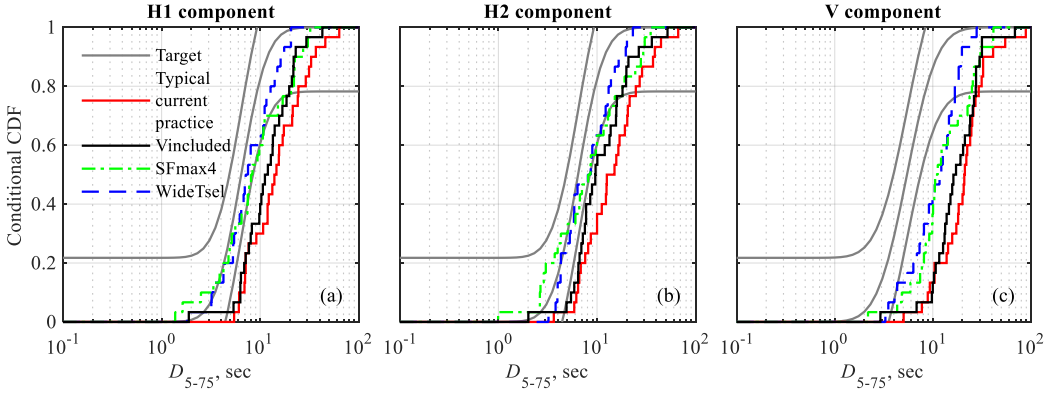

Fig. 7 – Evaluation of 5-75% significant duration for records selected from various versions of typical current practice: (a) H1, (b) H2, and (c) V components of GM.

The preceding hazard inconsistencies can be reduced by following any one of these three guidelines: (i) including the V component in the selection process, (ii) constraining the scale factors, or (iii) widening the period range for selecting GMs. To illustrate, three more ensembles of 30 GMs were selected to match the CS except each ensemble differs from the one depicted in Fig. 6 by only one aspect. For example, GMs were selected as in Fig. 6 except V components were included in the selection process via $w_H = 0.5$; the corresponding values of D_{5-75} are shown as solid black curves in Fig. 7, revealing a slight improvement in hazard consistency. Similarly, GMs were selected as in Fig. 6 except (i) scale factors were constrained to within 0.25 to 4 or (ii) the shaded period range for selection in Fig. 6a was widened to 0.01 to 10 sec; the values of D_{5-75} corresponding to these two independent changes are shown, respectively, by chained green and dashed blue curves in Fig. 7. Although Fig. 7 only shows D_{5-75}, each of the preceding three ensembles yielded improvements in terms of spectral accelerations as well (not shown due to space limitations). Ideally, all three

guidelines should be pursued (i.e., compare Figs. 4 and 5 against Figs. 6 and 7) but constraining scale factors may not be possible in some situations (e.g., lack of GMs available for a very long return period of interest).

4. Developing a USGS web-based tool

The proposed GM selection approach guarantees hazard consistency of multicomponent GMs with respect to spectral accelerations for all three components of GMs; furthermore, the selected GMs may also be hazard consistent with respect to other IMs. However, this approach requires first determining the target spectrum for the V component of GM, which is not as easily accessible to the profession compared to choosing a GM ensemble via engineering judgment and then conducting IDA. One way to provide an easily accessible alternative to IDA is by resurrecting the USGS web-based tool for the CS [52] and enhancing it to include the V component of GM. However, at least two more aspects require further exploration: (i) availability of GM models for other tectonic regimes when computing the CS (see Section 2) and (ii) influence on CS due to multiple earthquake scenarios and multiple GMPMs [52].

5. Conclusions

In this paper, the CS and the GM selection approach by Jayaram et al. [7] and Baker and Lee [10] were extended to include the V component of GM; software for computing the multicomponent target spectrum and subsequently selecting GMs is provided on GitHub. Moreover, the necessary ingredients for practical implementation of the CS were explicitly identified, informing future work on development of GMPMs, correlation models, and a USGS web-based tool. Using the target spectrum and the GM selection approach developed in this study, the typical current practice for selecting and scaling V components of GM is evaluated. The latter approach can yield hazard-inconsistent multicomponent GMs, but hazard consistency can be improved by (i) including the V component in the selection process, (ii) constraining the scale factors, or (iii) widening the period range for selecting GMs. When these three guidelines were simultaneously utilized, the resulting multicomponent GMs were observed to be hazard consistent with respect to IMs that were not used to select the GMs. This suggests that the proposed GM selection approach provides seismic risk estimates that are more accurate than those from existing approaches; however, this hypothesis should be investigated further in future research.

6. References

[1] Chopra AK (2017): *Dynamics of Structures: Theory and Applications to Earthquake Engineering*. Pearson Prentice Hall, 5th edition.

[2] NEHRP Consultants Joint Venture (2011): Selecting and scaling earthquake ground motions for performing response-history analyses. *Technical Report*, National Institute of Standards and Technology, Maryland, USA.

[3] Vamvatsikos D, Cornell CA (2002): Incremental dynamic analysis. *Earthquake Engineering & Structural Dynamics*, **31** (3), 491–514.

[4] Jalayer F (2003): Direct probabilistic seismic analysis: Implementing non-linear dynamic assessments. *PhD Thesis*, Stanford University, Stanford, USA.

[5] Baker JW (2015): Efficient analytical fragility function fitting using dynamic structural analysis. *Earthquake Spectra*, **31** (1), 579–599.

[6] Applied Technology Council (2009): Quantification of building seismic performance factors. *Technical Report FEMA P695*, Federal Emergency Management Agency, Washington DC, USA.

[7] Jayaram N, Lin T, Baker JW (2011): A computationally efficient ground-motion selection algorithm for matching a target response spectrum mean and variance. *Earthquake Spectra*, **27**(3), 797–815.

[8] Lin T, Haselton CB, Baker JW (2013): Conditional Spectrum-based ground motion selection. Part I: Hazard consistency for risk-based assessments. *Earthquake Engineering & Structural Dynamics*, **42**(12), 1847–1865.

[9] Kohrangi M, Bazzurro P, Vamvatsikos D (2016): Vector and scalar IMs in structural response estimation, Part II: Building demand assessment. *Earthquake Spectra*, **32**(3), 1525–1543.

[10] Baker JW, Lee C (2018): An improved algorithm for selecting ground motions to match a Conditional Spectrum. *Journal of Earthquake Engineering*, **22**(4), 708–723.

[11] Ryan KL, Dao ND (2015): Influence of vertical ground shaking on horizontal response of seismically isolated buildings with friction bearings. *Journal of Structural Engineering*, **142**(1), 4015089.

[12] Kunnath SK, Abrahamson NA, Chai YH, Erduran E, Yilmaz Z (2008): Development of guidelines for incorporation of vertical ground motion effects in seismic design of highway bridges. *Technical Report CA/UCD-SESM-08-01*, California Department of Transportation, Sacramento, USA.

[13] Løkke A, Chopra AK (2017): Direct finite element method for nonlinear analysis of semi-unbounded dam–water–foundation rock systems. *Earthquake Engineering & Structural Dynamics*, **46**(8), 1267–1285.

[14] Kumar M, Whittaker AS, Constantinou MC (2015): Seismic isolation of nuclear power plants using sliding bearings. *Technical Report*, Multidisciplinary Center for Earthquake Engineering Research, New York, USA.

[15] Hariri-Ardebili MA, Saouma VE (2016): Collapse fragility curves for concrete dams: Comprehensive study. *Journal of Structural Engineering*, **142**(10), 4016075.

[16] Bernier C, Padgett JE, Proulx J, Paultre P (2015): Seismic fragility of concrete gravity dams with spatial variation of angle of friction: Case study. *Journal of Structural Engineering*, **142**(5), 5015002.

[17] Harrington CC, Liel AB (2016): Collapse assessment of moment frame buildings, considering vertical ground shaking. *Earthquake Engineering & Structural Dynamics*, **45**(15), 2475–2493.

[18] PEER Tall Buildings Initiative (2017): Guidelines for performance-based seismic design of tall buildings. *Technical Report PEER 2017/06*, Pacific Earthquake Engineering Research, Berkeley, USA.

[19] Grigoriu M (2010): To scale or not to scale seismic ground-acceleration records. *Journal of Engineering Mechanics*, **137**(4), 284–293.

[20] Kwong NS, Chopra AK, McGuire RK (2015): A framework for the evaluation of ground motion selection and modification procedures. *Earthquake Engineering & Structural Dynamics*, **44**(5), 795–815.

[21] Bernier C, Monteiro R, Paultre P (2016): Using the Conditional Spectrum method for improved fragility assessment of concrete gravity dams in eastern Canada. *Earthquake Spectra*, **32**(3), 1449–1468.

[22] Dávalos H, Miranda E (2019): Evaluation of bias on the probability of collapse from amplitude scaling using spectral-shape-matched records. *Earthquake Engineering & Structural Dynamics*, **48**(8), 970–986.

[23] Gülerce Z, Abrahamson NA (2011): Site-specific design spectra for vertical ground motion. *Earthquake Spectra*, **27**(4), 1023–1047.

[24] Kwong NS, Chopra AK (2020): Selecting, scaling, and orienting three components of ground motions for intensity-based assessments at far-field sites. *Earthquake Spectra*, DOI: 10.1177/8755293019899954.

[25] Nievas C, Sullivan T (2018): A multidirectional Conditional Spectrum. *Earthquake Engineering & Structural Dynamics*, **47**(4), 945–965.

[26] Kohrangi M, Bazzurro P, Vamvatsikos D (2019): Conditional Spectrum bidirectional record selection for risk assessment of 3D structures using scalar and vector IMs. *Earthquake Engineering & Structural Dynamics*, **48**(9), 1066–1082.

[27] Jayaram N, Baker JW (2008): Statistical tests of the joint distribution of spectral acceleration values. *Bulletin of the Seismological Society of America*, **98**(5), 2231–2243.

[28] Baker JW, Lin T, Shahi SK (2011): New ground motion selection procedures and selected motions for the PEER transportation research program. *Technical Report PEER 2011/03*, Pacific Earthquake Engineering Research, Berkeley, USA.

[29] Campbell KW, Bozorgnia Y (2014): NGA-West2 ground motion model for the average horizontal components of PGA, PGV, and 5% damped linear acceleration response spectra. *Earthquake Spectra*, **30**(3), 1087–1115.

[30] Baker JW, Jayaram N (2008): Correlation of spectral acceleration values from NGA ground motion models.

Earthquake Spectra, **24**(1), 299–317.

[31] Baker JW, Cornell CA (2006): Correlation of response spectral values for multicomponent ground motions. *Bulletin of the Seismological Society of America*, **96**(1), 215–227.

[32] Boore DM (2010): Orientation-independent, nongeometric-mean measures of seismic intensity from two horizontal components of motion. *Bulletin of the Seismological Society of America*, **100**(4), 1830–1835.

[33] Bozorgnia Y *et al.* (2014): NGA-West2 research project. *Earthquake Spectra*, **30**(3), 973–987.

[34] Bozorgnia Y, Campbell KW (2016): Vertical ground motion model for PGA, PGV, and linear response spectra using the NGA-West2 database. *Earthquake Spectra*, **32**(2), 979–1004.

[35] Gülerce Z, Kamai R, Abrahamson NA, Silva WJ (2017): Ground motion prediction equations for the vertical ground motion component based on the NGA-W2 database. *Earthquake Spectra*, **33**(2), 499–528.

[36] Stewart JP, Boore DM, Seyhan E, Atkinson GM (2016): NGA-West2 equations for predicting vertical-component PGA, PGV, and 5%-damped PSA from shallow crustal earthquakes. *Earthquake Spectra*, **32**(2), 1005–1031.

[37] Bozorgnia Y, Campbell KW (2016): Ground motion model for the vertical-to-horizontal (V/H) ratios of PGA, PGV, and response spectra. *Earthquake Spectra*, **32**(2), 951–978.

[38] Wasserman L (2004): *All of Statistics: A Concise Course in Statistical Inference*. Springer.

[39] Baker JW, Cornell CA (2006): Spectral shape, epsilon and record selection. *Earthquake Engineering & Structural Dynamics*, **35**(9), 1077–1095.

[40] Kwong NS, Chopra AK (2017): A generalized Conditional Mean Spectrum and its application for intensity-based assessments of seismic demands. *Earthquake Spectra*, **33**(1), 123–143.

[41] ASCE Structural Engineering Institute (2017): Minimum design loads and associated criteria for buildings and other structures. *ASCE Standard 7-16*, American Society of Civil Engineers, Reston, USA.

[42] Bradley BA (2012): A ground motion selection algorithm based on the generalized conditional intensity measure approach. *Soil Dynamics and Earthquake Engineering*, **40**, 48–61.

[43] Higham NJ (1988): Computing a nearest symmetric positive semidefinite matrix. *Linear Algebra and its Applications*, **103**, 103–118.

[44] Luco N, Cornell CA (2007): Structure-specific scalar intensity measures for near-source and ordinary earthquake ground motions. *Earthquake Spectra*, **23**(2), 357–392.

[45] Bradley BA (2012): The seismic demand hazard and importance of the conditioning intensity measure. *Earthquake Engineering & Structural Dynamics*, **41**(11), 1417–1437.

[46] Jalayer F, Beck JL, Zareian F (2012): Analyzing the sufficiency of alternative scalar and vector intensity measures of ground shaking based on information theory. *Journal of Engineering Mechanics*, **138**(3), 307–316.

[47] Padgett JE, Nielson BG, DesRoches R (2008): Selection of optimal intensity measures in probabilistic seismic demand models of highway bridge portfolios. *Earthquake Engineering & Structural Dynamics*, **37**(5), 711–725.

[48] Bommer JJ, Stafford PJ, Alarcón JE (2009): Empirical equations for the prediction of the significant, bracketed, and uniform duration of earthquake ground motion. *Bulletin of the Seismological Society of America*, **99**(6), 3217–3233.

[49] Kramer SL (1996): *Geotechnical Earthquake Engineering*. Prentice Hall.

[50] Bradley BA (2010): A generalized conditional intensity measure approach and holistic ground-motion selection. *Earthquake Engineering & Structural Dynamics*, **39**(12), 1321–1342.

[51] Bradley BA (2011): Correlation of significant duration with amplitude and cumulative intensity measures and its use in ground motion selection. *Journal of Earthquake Engineering*, **15**(6), 809–832.

[52] Lin T, Harmsen SC, Baker JW, Luco N (2013): Conditional Spectrum computation incorporating multiple causal earthquakes and ground-motion prediction models. *Bulletin of the Seismological Society of America*, **103**(2A), 1103–1116.